



Interleukin-7-loaded oncolytic adenovirus improves CAR-T cell therapy for glioblastoma

Jianhan Huang¹ · Meijun Zheng² · Zongliang Zhang³ · Xin Tang¹ · Yaxing Chen¹ · Aijun Peng¹ · Xingchen Peng³ · Aiping Tong³ · Liangxue Zhou¹

Received: 13 September 2020 / Accepted: 6 January 2021 / Published online: 4 February 2021
© The Author(s), under exclusive licence to Springer-Verlag GmbH, DE part of Springer Nature 2021

Abstract

Background T cell with chimeric antigen receptors (CAR-T) has presented remarkable efficacy for blood cancer as an emerging immunotherapy. However, for solid tumors, the therapeutic efficacy is much impaired due to the lack of infiltration and persistence of CAR-T in tumor tissue. Thus, we constructed an interleukin-7-loaded oncolytic adenovirus and combined the use of oncolytic virus and CAR-T to improve the therapeutic outcome.

Methods We constructed an interleukin-7-loaded oncolytic adenovirus (oAD-IL7) and a B7H3-targeted CAR-T and explored the efficacy of the single use of oAD-IL7, B7H3-CAR-T, or the combined therapy for glioblastoma in vitro and in vivo. The improved CAR-T anti-tumor efficacy was evaluated according to the proliferation, survival, persistence, exhaustion of T cells, and tumor regression.

Results Constructed oAD-IL7 and B7H3-CAR-T presented moderate cytotoxicity during in vitro study, but failed to induce a thorough and persistent anti-tumor therapeutic efficacy in vivo. The combination of oAD-IL7 and B7H3-CAR-T in vitro resulted in enhanced T cell proliferation and reduced T cell apoptosis. The joint efficacy was further confirmed using tumor-bearing xenograft mice. During in vivo study, the mice treated with both oAD-IL7 and B7H3-CAR-T showed prolonged survival and reduced tumor burden. According to the ex vivo study, oAD-IL7 improved the proliferation and persistence of tumor-infiltrating B7H3-CAR-T, but failed to reverse the exhaustion.

Conclusions Our results indicated that oAD-IL7 is a promising auxiliary therapy to improve the therapeutic efficacy of B7H3-CAR-T in glioblastoma by providing the activating signals for tumor-infiltrating T cells. Our results also lay the basis for the future clinical trials for the combination of IL7-loaded oncolytic adenovirus and CAR-T therapy for glioblastoma.

Keywords CAR · Oncolytic virus · IL7 · B7H3 · Cancer

Abbreviations

CAR-T Chimeric antigen receptor T cells
DAMPs Damage-associated molecular patterns
GBM Glioblastoma

IL7 Interleukin-7
MDSC Myeloid-derived suppressor cells
oAD Oncolytic adenovirus
PAMPs Pathogen-associated molecular patterns
scFv Single-chain variable fragment

Jianhan Huang and Meijun Zheng have contributed equally to this work.

✉ Aiping Tong
aipingtong@scu.edu.cn

✉ Liangxue Zhou
liangxue_zhou@126.com

¹ Department of Neurosurgery, West China Hospital, West China Medical School, Sichuan University, No. 37 Guo Xue Xiang, Chengdu 610041, Sichuan Province, People's Republic of China

² Department of Otolaryngology, Head and Neck Surgery, West China Hospital, West China Medical School, Sichuan

University, No. 37 Guo Xue Xiang, Chengdu 610041, Sichuan Province, People's Republic of China

³ State Key Laboratory of Biotherapy, West China Hospital, West China Medical School, Sichuan University, No. 37 Guo Xue Xiang, Chengdu 610041, Sichuan Province, People's Republic of China

Background

Chimeric antigen receptor T cell therapy (CAR-T) is a promising immunotherapy for cancer treatment [1]. Consisting of an immunoglobulin single-chain variable fragment (scFv) that binds the target antigen, a transmembrane domain, and intracellular T cell signaling domains, the manual chimeric antigen receptor enables CAR-T to recognize tumor cells with specific targets and provides CAR-T with the first and second activation signals. So far, two CAR-T products, Kymriah and Yescarta, have been approved by the Food and Drug Administration (FDA) and have achieved great success in the treatment of relapse and refractory B cell non-Hodgkin's lymphoma and acute lymphoblastic leukemia [2]. However, for solid tumors, CAR-T therapy only gets limited therapeutic efficacy [3]. Different from that in hematologic cancer, the tumor microenvironment in solid tumors, which includes Treg, myeloid-derived suppressor cells (MDSC), fibroblast, and the subsequent immunosuppressive cytokines, induces rapid T cell exhaustion and reduced T cell survival [4]. To improve the therapeutic efficacy of CAR-T cells, multiple studies have been made to provide the CAR-T cells with essential supplements which is indispensable for the consistent proliferation and long-term survival of tumor-infiltrating CAR-T cells, such as directly modifying CAR-T cells with self-secreting cytokines or taking use of auxiliary therapy to reverse the immunosuppressive tumor microenvironment [5, 6].

Oncolytic virus is a promising therapy in cancer treatment, especially as an auxiliary for tumor immunotherapy [7]. Different from traditional chemotherapeutic drugs or targeted therapy, in addition to the direct tumor lysis efficacy, the virus ingredients were recognized by innate immune system as pathogen-associated molecular patterns (PAMPs), which combines with damage-associated molecular patterns (DAMPs) and tumor-specific antigens released by infected tumor cells and leads to a strong immuno-activating effect similar in virus infection diseases [8]. Moreover, after modifying the oncolytic virus with coding sequence of gene therapy agents, the tumor restricted replication of oncolytic virus results in local release of loaded products [9]. This property of oncolytic virus makes it a safe and effective tool for the delivery of a series of powerful immuno-activators which are usually accompanied by serious toxicity when applied systematically, such as different types of interleukins [10, 11].

Interleukin-7 (IL7) is a cytokine produced by marrow stromal cells and thymic epithelial cells and has been supposed to be one of the most important cytokines for the long-term survival of tumor-infiltrating T cells [12]. Several pre-clinical studies have tried to equipped

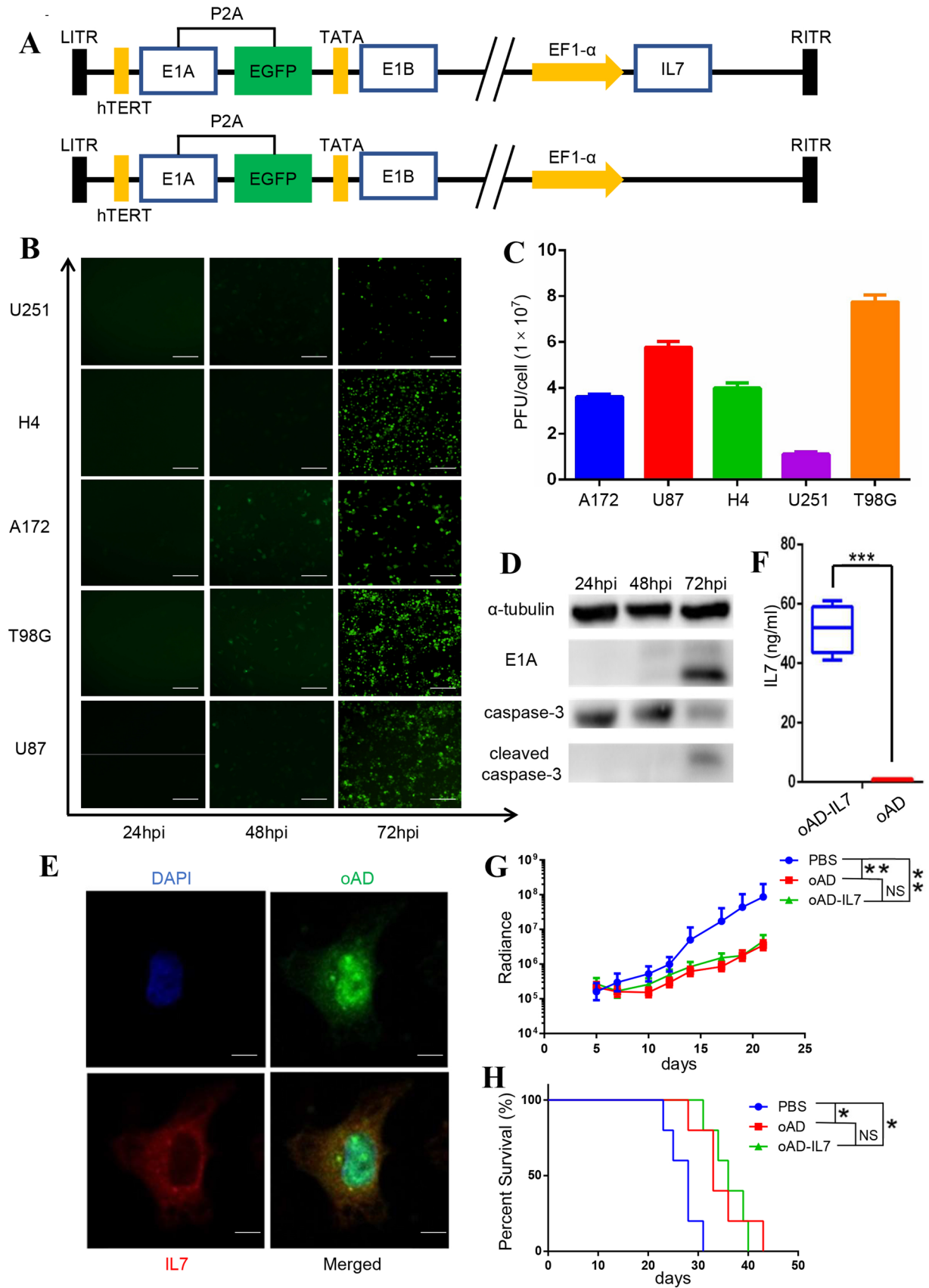
Fig. 1 oAD-IL7 successfully replicate in glioma. **a** Schematic representation of genome of the oncolytic viruses used in this study. **b** Monolayers of glioblastoma cell lines were infected by oAD-IL7 at the MOI of 10. Cells were imaged with a fluorescence microscope 24, 48, and 72 h after infection. Scale bar, 500 μm . **c** Cells were collected 72 h after infection for plaque assay. Each number of the virus titer were calculated on average of three independent wells. **d** Oncolytic virus-induced GBM apoptosis was confirmed by western blot. Scale bar, 100 μm . **e** Cells were stained with IL7 antibody 72 h after infection and imaged with a fluorescence microscope. Green fluorescence represents the oAD-IL7 infection; red fluorescence represents the IL7 distribution; blue fluorescence represents the cell nuclei stained with DAPI. Scale bar, 50 nm. **f** Supernatants were collected for IL7 quantification. **g** The median tumor volume of the xenograft models treated by PBS, oAD, and oAD-IL7 was recorded. **h** Survival analysis of the three group of the xenograft models. * $P < 0.05$; ** $P < 0.01$; *** $P < 0.001$ (two-tailed paired t test)

tumor-infiltrating CAR-T cells with IL7, such as modifying CAR-T cells with auto-secreting IL7, or taking use of IL7 engineered mesenchymal stem cells to provide IL7 signal for CAR-T [13, 14]. Here, we constructed an oncolytic adenovirus loaded with IL7 (oAD-IL7) and combined it with B7H3-targeting CAR-T cells to explore their joint efficacy for glioblastoma treatment. Our results showed that the oAD-IL7 improved the therapeutic efficacy of CAR-T cells for glioblastoma in vitro and in vivo by improving the survival and proliferation of tumor-infiltrating CAR-T cells.

Materials and methods

Cells

293 T, 293A, and four types of glioblastoma (GBM) cell lines, including U87, U251, A172, and T98G, were purchased from ATCC. Another GBM cell line H4 is a kind gift from Sheng Zenghua in our laboratory. 293 T, 293A, U87, U251, A172, H4, and T98G were maintained in DMEM (Gibco), supplemented with 10% FBS (Gemini), penicillin (100U/ml), and streptomycin (100 $\mu\text{g}/\text{ml}$). For in vivo imaging, patient-derived glioblastoma tissue were dissolved using 1% collagenase (Solarbio) and then cultured in an incubator at 37 $^{\circ}\text{C}$. Six days later, primary glioblastoma cells were modified to express luciferase by lentivirus transduction and named GBM19-LUCF after puromycin selection. Primary tumor samples obtained from patients with GBM and blood samples from GBM patients and healthy donors were also approved by West China Hospital of Sichuan University Biomedical Ethics Committee (ethical approval document 2018-061). Written informed consent was obtained from patients with GBM and healthy donors.



Adenovirus construction

The schematic representation of oAD-IL7 and its blank counterpart is shown in Fig. 1. Both oncolytic adenovirus were based on ADMAX system, which consists of an E1, E3-deleted serotype 5 human adenovirus backbone, pBHglox Δ E1,E3, and a shuttle plasmid, pDC316-EGFP. A cDNA encoding human IL7 purchased from Sinobiological (Beijing, China) was cloned and then inserted the E1 region, and an E1A gene under the control of hTERT, followed by a E1B gene under the control of TATA box was synthesized by General Biosystems (Chuzhou, Anhui province, China) and inserted into the E3 region. The two types of viruses were rescued from 293A cells 7 days after transduction of the modified backbone and shuttle plasmids for further experiment by three consecutive freeze–thaw cycles. The titration was conducted using plaque assay. Briefly, monolayer 293A cells were infected by gradient-diluted viral solutions. Four h later, the infection media were replaced by overlay media consisting of DMEM (Gibco), 0.8% agarose (Sangon Biotech), and 2% FBS (Gemini). The GFP-positive plaques were counted using a fluorescence microscope (Zeiss, Axio observer Z1) 3 days later. Finally, the viruses were purified by cesium chloride gradient centrifugation.

T cell generation

Primary lymphocytes were kindly donated by healthy donors in our laboratory and were isolated by gradient centrifugation at a speed of 800 g for 15 min. Purified T cells were then cultured in 24-well plate in X-vivo media (Lonza) with 10% FBS, 100 U/ml penicillin, 100 μ g/ml streptomycin at a density of 1×10^6 cells/ml in a 37 °C incubator with an atmosphere containing 5% CO₂. 100 U/ml interleukin-2 (Life Science), 5 ng/ml IL15 (Miltenyi), and CD3/CD28 T cell transact (Miltenyi) were added for T cell activation and sustaining. 72 h later, the activated T cells were transduced by lentivirus at an MOI of 10, with the assistance of 10 μ g/well coated retronectin (Takara) in the presence of IL-2. After 12 h incubation, the T cells were collected and maintained in daily refreshed media (X-vivo, Lonza) with 100 U/ml IL-2, until the following experiment 6–8 days later. The titration of the lentivirus is conducted using TCID50 assay.

Immunofluorescent staining and western blot

Immunofluorescent staining and western blot analysis were conducted as previously described [15]. For western blot, 1×10^6 /well U87 cells were incubated in 6-well plate for 12 h. Then 1×10^7 oncolytic adenovirus were added to each well. The cells were collected 24, 48, and 72 h after viral infection and lysed for protein extraction and further experiment. For immunofluorescent staining, 1×10^5 /well

GBM cells were incubated in 24-well plate with poly-L-lysine-treated coverlips for 12 h, and then, adenoviral infection was performed at an MOI of 1. The specimens were incubated in 4% paraformaldehyde followed by 0.1% Triton X-100 incubation for 20 min and then stained with anti-IL7 and DAPI (Beyotime). The images were captured by confocal microscopy (Zeiss, AXIO observer Z1).

Flow cytometry

For each flow cytometry specimen, 1×10^6 cells were twice washed by PBS and then incubated in 1% BSA solution with Fc blocker (Biolegend) for 30 min. For ki67 staining, the specimens were fixed and perforated for another hour using BD Cytofix/Cytoperm™ kit after surface staining. Fluorochrome-conjugated antibodies were purchase from Biolegend (CD3, CD4, CD8, CD25, CD69, PD1, LAG3), Huabio (IL7), and BD (CD19, B7H3, ki67). T cell activation analysis were performed using FlowJo 9.3.2, while the transduction efficiency of CAR-T, B7H3 expression on GBM cells, and proliferation assay were measured by ACEA NovoCyte (Agilent Biosciences).

T cell activation, cytokine secretion, and cytotoxicity

2×10^5 U87 cells were seeded in 24-well plate overnight and cocultured with CAR-T cells for 48 h. For activation analysis, T cells were collected and stained with CD3, CD4, CD8, CD25, and CD69 for flow cytometry. For cytokine secretion analysis, supernatants were harvested for TNF- α and IFN- γ quantitation by Elisa (R&D). For cytotoxicity assessment, the U87 cells were incubated in culture media with 0.5 mg/ml MTT reagent (Sangon, E606334-0500) for 4 h at 37 °C. Then the media was carefully aspirated, and 100 μ l formazan solubilization solution was added. Ten min later, the cytotoxicity was measured according to the absorbance at 570 nm.

CytoTel Blue proliferation assay

2×10^5 U87 cells were incubated in 24-well plate overnight, and then, viral infection was conducted at an MOI of 1. Twenty-four h later, the U87 cells were cocultured with 1×10^6 T cells for 3 days, and then, the T cells were collected for another round of proliferation assay until the day of 7. T cells were labeled with CytoTel Blue (AAT Bioquest) according to manufacturer's instruction before coculturing. At day 3, 5, and 7, the T cells were collected for proliferation analysis by using ACEA NovoCyte (Agilent Biosciences).

Apoptosis analysis

On the day 7 of coculture, cells were collected and stained with Annexin V and 7-AAD and analyzed by flow cytometry. Anti-CD3 fluorescent-conjugated antibody (Biolegend) was added to separate the T cells and U87 cells.

In vivo experiment

All animal experiments followed a protocol approved by the Institutional Animal Care and Use Committee of Sichuan University. All xenograft models were constructed based on six- to eight-week-old NCG mice, which were purchased from GemPharmatech and were bred in the animal vivarium at the State Key Laboratory of Biotherapy, Sichuan University, in a pathogen-free condition.

Xenograft models

Xenograft models were established by intracranial injection of 2×10^5 GBM-LUCF cells suspended in 5 μ l PBS solution for each mouse into the right frontal lobe of the brain located in 2 mm lateral and 1 mm anterior to bregma at a depth of 3 mm. Seven days later, xenografts were confirmed by bioluminescent imaging and treated with an intratumoral injection of 1×10^8 pfu oAD-IL7 or oAD, respectively, into the same position aforementioned. B7H3-CAR-T cells were intravenously administered 2 days after viral injection. Tumors were captured twice a week by bioluminescent imaging, and the bioluminescent signals for each group were recorded using the IVIS system (Caliper Life Sciences). Mouse death served as the endpoint of the experiment.

Bioluminescent imaging

GBM19 cells expressing luciferase were used to detect tumor growth during in vivo experiment. The mice were treated with intraperitoneal injection of 150 mg/kg D-luciferin (Beyotime) dissolved in PBS. Bioluminescent imaging was performed using the IVIS system (Caliper Life Sciences) 10 min after D-luciferin injection, and the radiance of tumor region was recorded for each mouse.

Ex vivo experiment

Mice underwent delayed treatment were killed, and the tumors were harvested 7 days after B7H3-CAR-T administration. For H&E stain, the specimens were fixed in 4% formaldehyde for 24 h. For cytometry analysis, the tumors

were incubated in 1% collagenase for 1 h and washed by PBS twice.

Immunohistochemistry

Tumor specimens were harvested at the experiment endpoint or removed from GBM patients and embedded in paraffin. For tumor-infiltrating B7H3-CAR-T detection, sections were stained with anti-CD3 (Cell Signaling Technology, D4V8L). For B7H3 and CXAR, sections were stained with anti-B7H3 (Cell Signaling Technology, D9M2L) and anti-CXAR (Cell Signaling Technology, D3W3G).

Statistics

During in vitro assay, three wells were set as a group, and the experiments were repeated for twice. Significance was determined by two-sided Student's unpaired *t* tests. The survival curve was obtained by Kaplan–Meier plot, and a two-sided log rank test was applied for mouse survival test. $P < 0.05$ was considered as significant ($*P < 0.05$; $**P < 0.01$; $***P < 0.001$). All the statistics were performed using GraphPad Prism v6.04.

Results

Modified oncolytic adenovirus successfully propagates in GBM cells and produces IL7

We generated a type V oncolytic adenovirus with a E1A gene under the control of an hTERT promoter and the coding sequence of IL7, together with its blank control (Fig. 1a) [16]. oAD-IL7 and blank oAD successfully infected and replicated in all the 5 types of GBM cell lines (Fig. 1b), during which the IL7-carrying oncolytic virus presented similar replication capability compared with its blank control (supplementary fig. 1a–e). We next titrated the exact virus copies by plaque assay for consecutive collection of infected GBM cells, in which the viral replication grew fastest in U87 and T98G while much attenuated in U251 (Fig. 1c). The cytotoxicity of oAD-IL7 was confirmed by the increased cleaved caspase-3 in infected tumor cells, which was parallel to the viral replication as presented by accumulated E1A protein (Fig. 1d). The therapeutic efficacy of the oAD and oAD-IL7 for different glioblastoma cell lines was further quantified by MTT results after infecting the cell lines at different MOI (Supplementary figure 2), which differed among different glioblastoma cell lines. To confirm the expression of IL7 by infected GBM cells, immunofluorescence was performed 72 h after the viral infection to capture the secretion of IL7 (Fig. 1e). The soluble IL7 in the collected supernatant was quantified by Elisa assay (Fig. 1f). We conducted a xenograft

model based on U87 cell lines to verify the *in vivo* therapeutic efficacy of the oAD and oAD-IL7. Both the viruses presented moderate anti-tumor effect, and we found there was no significant difference according to the tumor volume and the survival (Fig. 1g, h).

B7H3-CAR-T exerts selective cytotoxicity to B7H3-positive GBM cells

B7H3 is a promising target for glioblastoma treatment, which is found to prevail on nearly 70% of the tumor tissue removed from patients. In the previous research, we constructed a B7H3-targeting CAR-T, which was equipped with a B7H3-targeted chimeric antigen receptor (CAR) consisting of a JB7H3-scFv, a CD8 α transmembrane domain, and a 4-1BB signaling intracellular domain (Fig. 2a, supplementary table 1). This CAR-T product has been proved to be effective and safe in our previous research for a series of B7H3 positive tumors. To measure the transduction efficiency of CAR-T cells, we inserted a coding sequence of the extracellular domain of CD19 acting as a marker for flow cytometry analysis (Fig. 2b, supplementary fig. 3a). The level of B7H3 expression varied among the five types of GBM cell lines, with the highest on A172 (Fig. 2c). We also confirmed the enhanced expression of B7H3 and coxsackie–adenovirus receptor (CXAR) among glioblastoma tissue and its relationship with survival based on data collected from Gene Expression Profiling Interactive Analysis (GEPIA) web server (supplementary fig. 4). To test the function of the B7H3-CAR-T, we cocultured the CAR-T cells with the GBM cells at an E:T rates of 1:1 and 1:5. After 48 h coculturing, for CAR-T cells, the activation of T cells was confirmed according to the upregulation of CD25 and CD69 measured by flow cytometry, together with elevated IFN- γ and TNF- α levels detected by Elisa assay, in which the CAR-T significantly outperformed the untransduced T cells (Fig. 2d, f, supplementary fig. 3b). The expression of the IL7R (CD127), which is the basis of the improved therapeutic efficacy of the combined therapy, was also measured during flow cytometry analysis, in which about half of the B7H3-CAR-T cells presented positive (Fig. 2e). We next conducted a ^{51}Cr -release assay for the remaining tumor cells to measure the cytotoxicity of the B7H3-CAR-T against glioblastoma cell lines, in which the B7H3-CAR-T presented highest efficacy for the A172 cell lines but a least cytotoxicity for T98G (Fig. 2g).

oAD-IL7 enhanced the survival and efficacy of B7H3-CAR-T

We hypothesized that the oncolytic virus might act as an ideal carrier for the IL7 to support the survival and efficacy of tumor-infiltrating CAR-T cells. To test this, we conduct

a serial coculture for untransduced T cells and CAR-T cells with oAD or oAD-IL7 infected U87 cells for 7 days in total (Fig. 3a). The CAR-T cells were stained with CytoTell Blue and then cocultured with virus-infected U87 cells that were refreshed on day 4. According to cell number recorded for each day, the CAR-T cells exposed to oAD-IL7 outperformed their counterparts, especially in the second round of coculture that started at day 4 (Fig. 3b). We next assessed the promotion of oAD-IL7 to the proliferation and survival of CAR-T cells during coculture separately. For proliferation monitoring, we recorded the signals of CytoTell Blue by flow cytometry on days 3 and 7. During the coculturing, although the two groups presented similar activation level, 86.32% versus 80.63%, 25.94% of the B7H3-CAR-T cocultured with oAD-IL7-infected U87 underwent more divisions (Fig. 3c). To assess the promotion of oAD-IL7 to the survival of CAR-T cells, we collected the CAR-T cells at the end of day 7 and performed an Annexin V /7-AAD staining, in which the CAR-T cells exposed to oAD-IL7 presented much lower rate of Annexin V $^{+}$ /7-AAD $^{+}$, and higher rate of Annexin V $^{-}$ /7-AAD $^{-}$ staining, compared to the T cells cocultured with blank oAD-infected U87 cells (Fig. 3d). Finally, the tumor cells alive after the second round of serial coculture were calculated by ^{51}Cr release assay to measure the *in vitro* improved long-term efficacy of CAR-T when exposed to oAD-IL7 (Fig. 3e, supplementary figure 5).

Combination of oAD-IL7 and B7H3-CAR-T improved the anti-tumor effect *in vivo*

We next combined the use of oAD-IL7 and B7H3-CAR-T in GBM xenograft models to test their joint efficacy *in vivo*. A total of 15 mice were divided into three groups and were separately treated with oAD-IL7, B7H3-CAR-T, and both of them. To construct the GBM xenograft models, we modified a patient-derived GBM cells with luciferase gene by lentivirus transduction (GBM-LUCF) and inoculated 2×10^5 GBM-LUCF cells in each NOD prkdc $^{-/-}$ IL-2Rg $^{-/-}$ (NCG) mice by intracranial injection after 10 days culturing. Treatment started on day 7 after inoculation, with an intracranial injection of 1×10^8 PFU oncolytic adenovirus and a dose of systemically applied 1×10^6 CAR-T cells 2 days later (Fig. 4a). The expression of B7H3 and CXAR of the glioblastoma from patient were verified by immunohistochemical analysis (Fig. 4b). We monitored the growth of the tumors by *in vivo* imaging system twice a week, and the intensity of the bioluminescence signal for each mouse was recorded (Fig. 4c). Although the CXAR is expressed in the tumor tissue at high level, the remission of the constructed tumor was not significant (Fig. 4d). Meanwhile, the single use of CAR-T therapy led to a moderate but transient tumor reduction according to the radiance intensity, while the tumor soon relapsed since day 14 and finally led

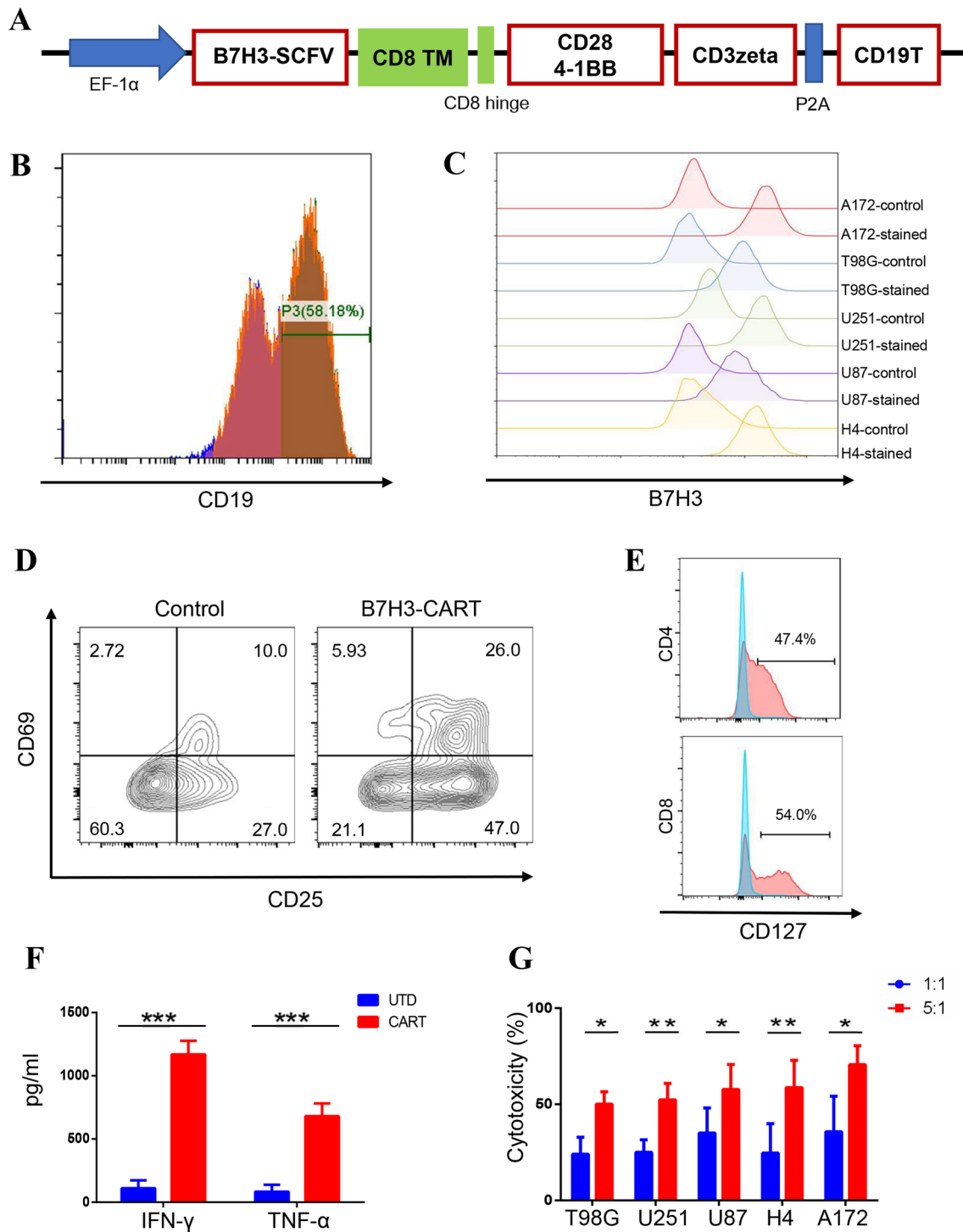


Fig. 2 B7H3-CAR-T exerts selective cytotoxicity to B7H3-positive GBM cells. **a** Schematic representation of B7H3-CAR. **b** Transduction efficiency of B7H3-CAR-T was calculated by flow cytometry 48 h after lentivirus infection. **c** Different GBM cell lines were stained with anti-B7H3 to calculate the levels of B7H3 expression. **d** B7H3-CAR-T and untransduced T cells were collected and stained with CD25 and CD69 after coculturing with U87 for 48 h (E:T = 5:1).

e Expression of the IL7R (CD127) on the modified B7H3-CAR-T cells. **f** Supernatants were obtained after 48 h coculturing (E:T = 5:1), and the concentration of TNF- α and IFN- γ were analyzed by Elisa assay. **g** ^{51}Cr -release assays were used to evaluate the lysis of GBM cells after treated with T cells at an E:T rate of 5:1 or 1:1. Representative results from three independent experiments are shown. * P < 0.05; ** P < 0.01; *** P < 0.001 (two-tailed paired t test)

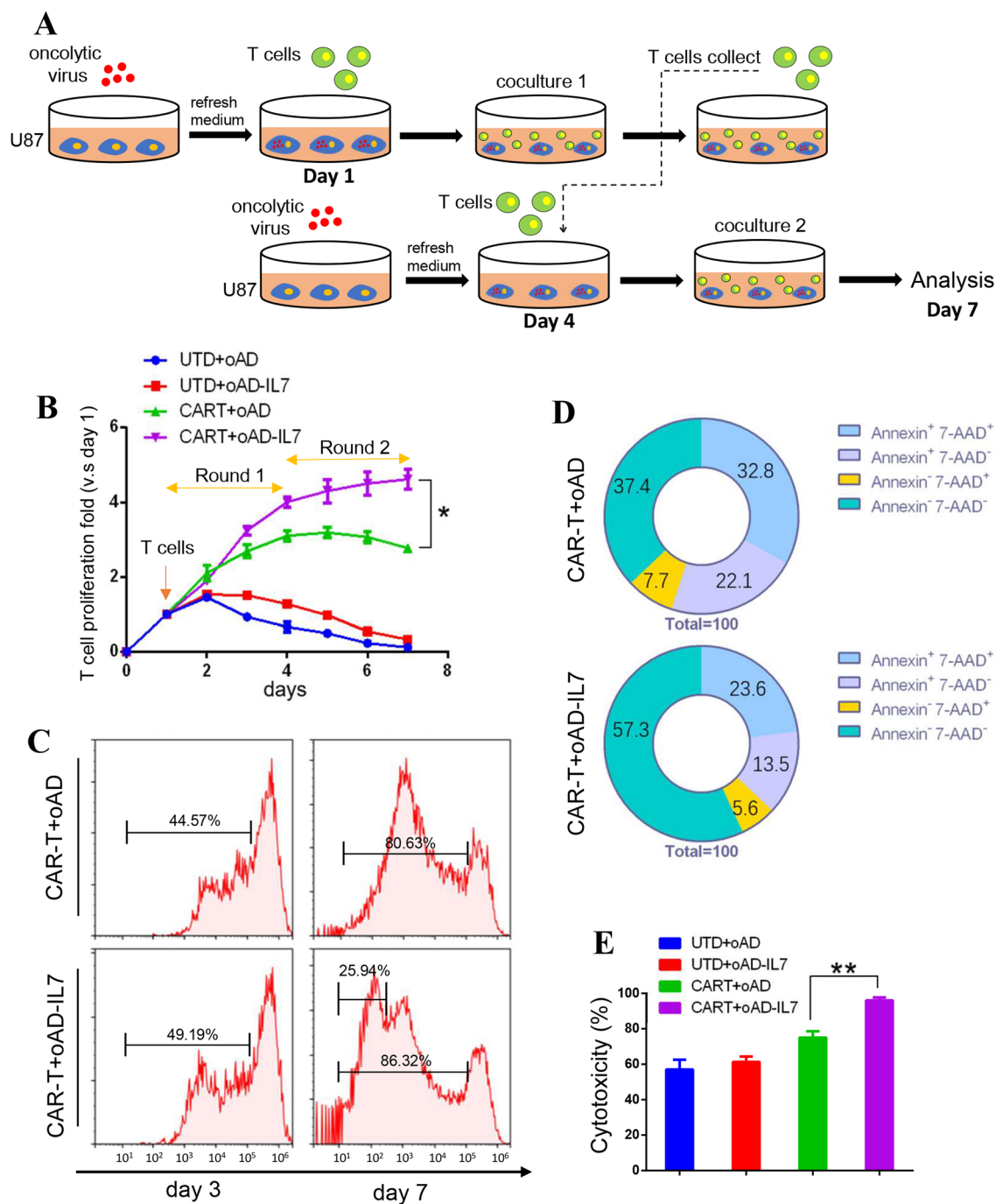


Fig. 3 oAD-IL7 enhanced the survival and efficacy of B7H3-CAR-T. **a** 1×10^5 B7H3-CAR-T or untransduced T cells underwent serial coculturing with 2×10^5 oncolytic virus-infected U87 cells for a total of 7 days. The GBM cells were refreshed on the 4th day of the serial coculture. **b** Cumulations of T cells expansion. **c** For proliferation analysis, T cells were stained with CytoTell Blue before serial cocul-

ture and collected for flow cytometry at the end of day 3 and day 7 to monitor the results of division. **d** For survival analysis, T cells were collected and stained with Annexin V and 7-AAD. **e** ^{51}Cr -release assays were used to evaluate the lysis of GBM during the second round of coculture at the end of day 7. Data represent the mean \pm SD of triplicate wells. * $P < 0.05$; ** $P < 0.01$ (two-tailed paired t test)

to the death of all the tumor-bearing mice (Fig. 4e). Finally, the combination of oAD-IL7 and B7H3-CAR-T presented significantly improved therapeutic efficacy, as the tumor-bearing mice got a consistent tumor regression, and four

out of five mice achieved long-term survival by the end of observation, day 60 (Fig. 4f–h). These results showed that the single use of either oncolytic adenovirus or CAR-T only brought limited therapeutic efficacy to tumor treatment, and

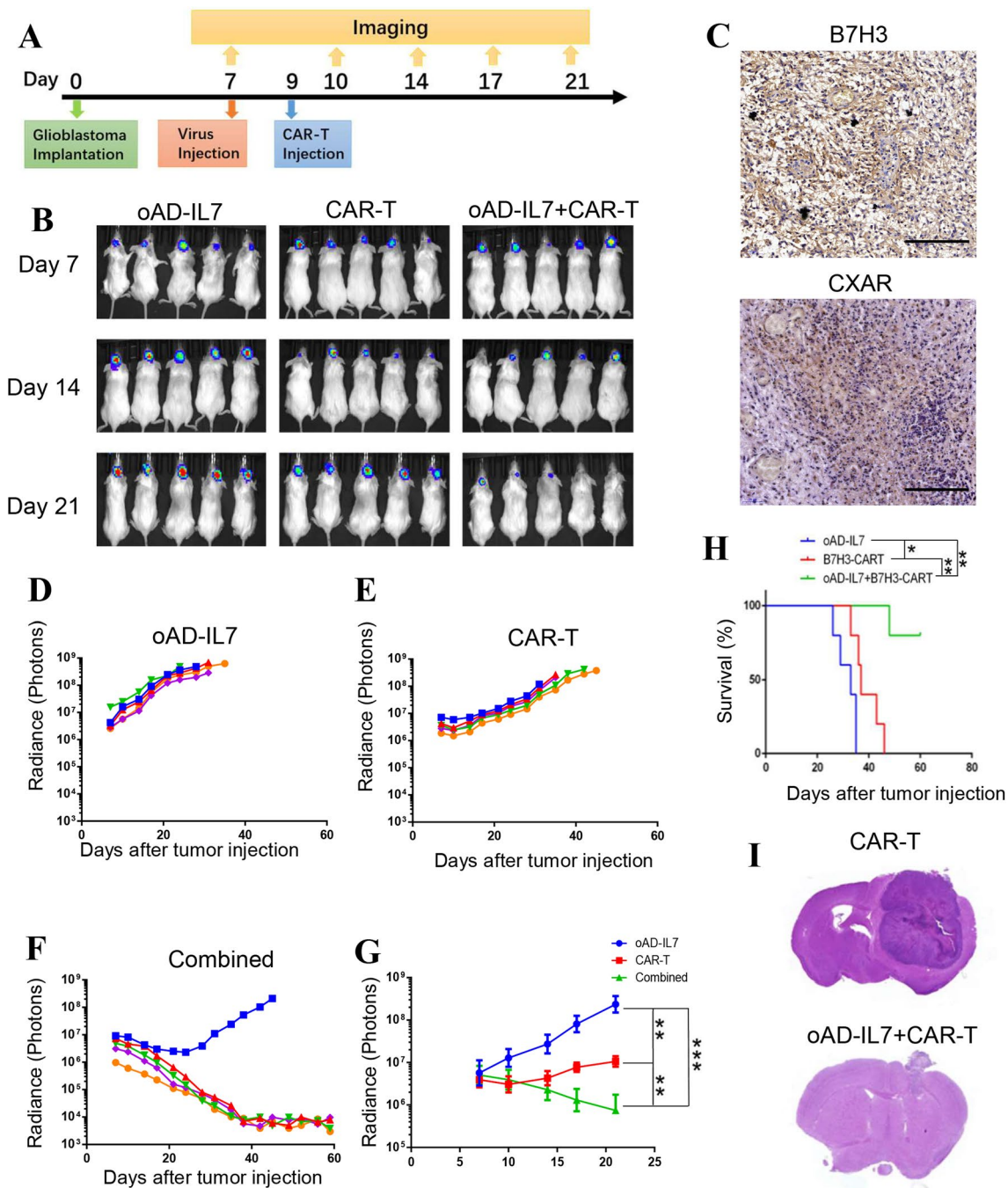
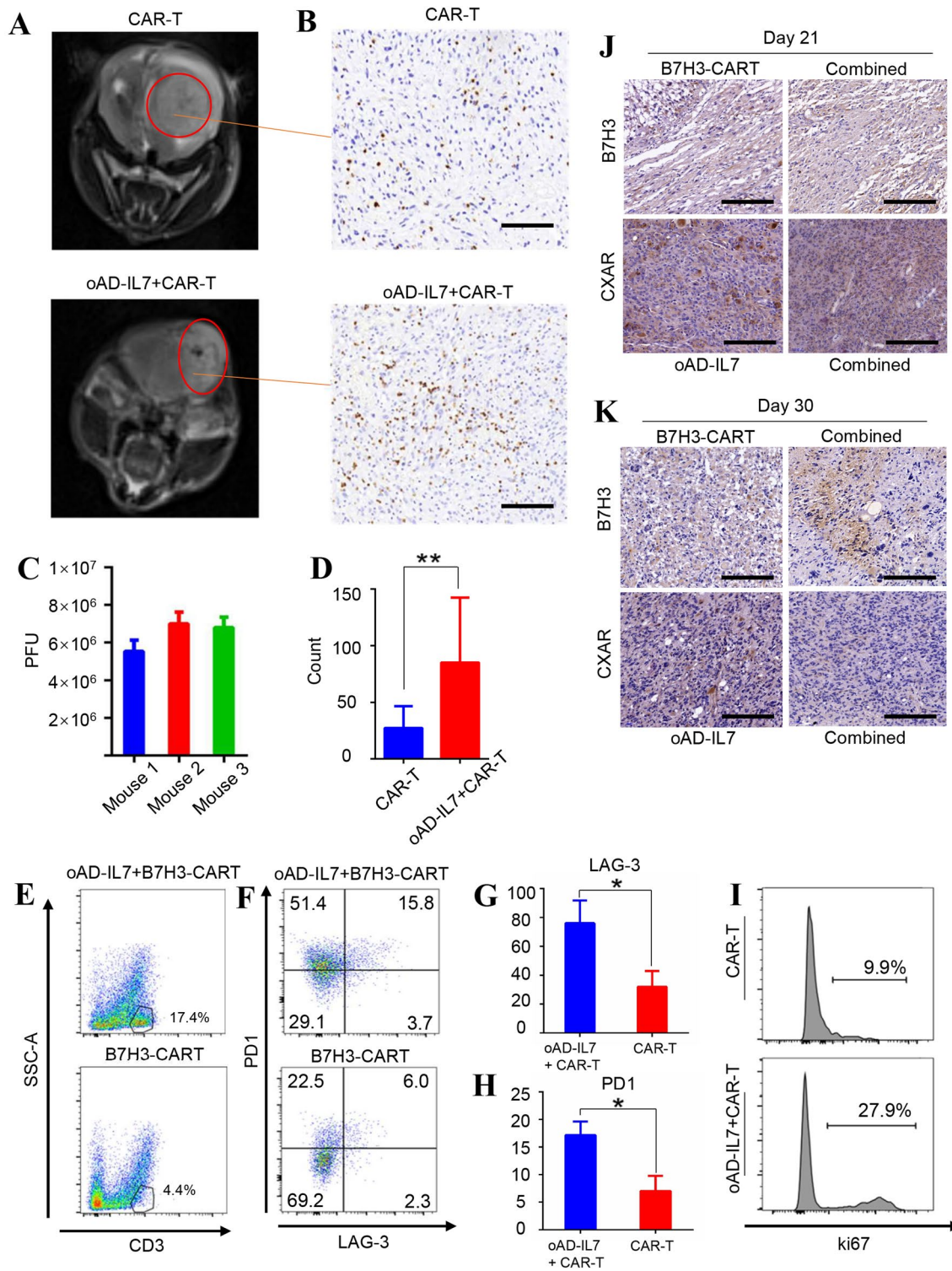


Fig. 4 Combination of oAD-IL7 and B7H3-CAR-T improved the anti-tumor effect in vivo. 2×10^5 GBM-LUCF cells were orthotopically injected into the NCG mice, and the bioluminescent imaging was performed twice a week since the 7th day after injection. The oncolytic virus was orthotopically injected on day 7, and the B7H3-CAR-T cells were systematically applied on day 9. **a** Experimental timeline for in vivo studies. **b** The representative bioluminescent images of the growth of glioblastoma over time were shown. **c** The expression of B7H3 and CXAR in the glioblastoma tissue of patient.

Scale bar, 50 μ m. **d**, **e**, and **f** Quantitated GBM-LUCF bioluminescence from each treatment group is displayed over time. **g** Average radiance of the three groups of the mice during the first 3 weeks. **h** Kaplan–Meier survival analysis of GBM-LUCF challenged mice after treatment with oncolytic virus and T cells. * $P < 0.05$; ** $P < 0.01$; *** $P < 0.001$ (two-tailed paired t test). **i** H&E staining of the specimen removed from tumor-bearing mice that underwent a parallel experiment at day 30

only the combined use of both of them induced a long-term and thorough anti-tumor effect. In a parallel experiment, the tumors were removed from the xenograft models on day

30 to verify the therapeutic effect, in which the combined group presented a much less tumor volume compared to its counterpart (Fig. 4i).



oAD-IL7 prolonged the survival of tumor-infiltrating CAR-T cells in xenograft models

To certify the improved persistence and proliferation of the CAR-T cells when used together with oAD-IL7, we next conducted another set of xenograft model and

delayed the treatment for the tumor-bearing mice to monitor the contributive effect of oAD-IL7 to the B7H3-CAR-T. For mice receiving combined therapies, the local injection of oncolytic virus was conducted on day 21 after inoculation, with CAR-T cells injected 2 days later for all mice. This delayed treatment lead to reduced

Fig. 5 oAD-IL7 prolonged the survival of tumor-infiltrating CAR-T cells in xenograft models. In a parallel experiment, the tumor-bearing mice underwent a delayed treatment since the 21st day after tumor inoculation. **a** The tumors of the mice treated with single B7H3-CAR-T therapy or combined therapy were imaged by MRI scanning at day 28. **b** The tumors were removed from the treated mice at day 30, and the immune infiltrate was evaluated by immunohistochemical staining according to the distribution of CD3⁺ cells. Scale bar, 200 μ m. **c** Titration of oAD-IL7 in glioblastoma tissue by plaque assay. **d** The ratio of CD3 positive cells in tumor tissues removed from mice treated by combined therapy or single B7H3-CAR-T therapy according to the count of average CD3⁺ cells in each single field. **e** Representative flow cytometry analysis of the T cells in the tumor removed from mice underwent different therapies. **f** The expression of PD1 and LAG-3 of the CD3 positive cells in two groups. **g** The level of LAG-3 expression on the tumor-infiltrating T cells of two groups. **h** The level of PD1 expression on the tumor-infiltrating T cells of two groups. **i** Ki67 expression of the CD3 positive cells in two groups. **j** Expression of the B7H3 and CXAR of the tumors removed from tumor-bearing mice on day 21. Scale bar, 50 μ m. **k** Expression of the B7H3 and CXAR of the tumors removed from tumor-bearing mice on day 30. Scale bar, 50 μ m

and incomplete tumor relieves. To evaluate the promotive efficacy of oAD-IL7 for infiltrating CAR-T cells, tumors were captured using MRI, in which the tumor-bearing mice treated with combined therapy showed significantly improved tumor relief compared to their counterparts treated with single CAR-T therapy (Fig. 5a) and then removed from the mice for immunohistology stain, virus detection, and flow cytometry analysis 7 days after CAR-T cell injection (Fig. 5b–d, supplementary figure 6). The number of the tumor-infiltrating CAR-T was measured according to the average count of CD3 positive cells in each field of the immunohistochemical analysis, in which the combined therapy led to a significant increase by approximately 3 times (85.2 vs 27.3) as much as the single use of B7H3-CAR-T (Fig. 5d). Next, we conducted a flow cytometry analysis for the tumor-infiltrating T cells, in which these tumor-infiltrating CAR-T cells presented improved activation and proliferation according to the elevated PD1, LAG-3, and ki67 expression (Fig. 5e–i). Further, we conducted an immunohistochemical analysis for the B7H3 and CXAR in the tumors removed from tumor-bearing mice of two group, which were collected on day 21 and 30. The B7H3 level of the xenograft tumor did not show significant decrease during the single B7H3-CAR-T treatment, compared to its counterpart in the combined group. Besides, the CXAR also presented a moderate decrease in the combined group compared to its counterpart (Fig. 5j, k). These results indicated that the lack of therapeutic efficacy of single B7H3-CAR-T was mainly attributed to the incomplete anti-tumor efficacy of the B7H3-CAR-T in the late stage of the tumor, and the heterogeneity of the tumor played an important role during the recurrence of the tumor.

Discussion

Apart from the activation of CD3 and CD28 pathway, the stimulation from interleukins have long been regarded as the third necessary signal for T cell homeostasis [17]. Considering the supplement of interleukins led to the prolonged survival of T cells during the in vitro T cell cultivation, in recent years there were a series of attempts to provide tumor-infiltrating CAR-T with different kinds of interleukins to prolong the persistence and therapeutic efficacy of the CAR-T against solid tumor [6, 18]. In this research, we constructed an IL7 carrying oncolytic virus and a B7H3-targeting CAR-T therapy and verified the promotive efficacy of oAD-IL7 for B7H3-CAR-T in an orthotopic glioblastoma model. Our results showed that oAD-IL7 promoted the proliferation and survival of B7H3-CAR-T both in vitro and in vivo and induced an improved anti-tumor efficacy compared with single B7H3-CAR-T therapy according to the prolonged survival of mice undergoing combined therapy.

We constructed the oAD-IL7 in which the E1A gene was under the control of an hTERT promoter and examined the anti-tumor efficacy of the constructed oAD-IL7 both in vitro and, as a control group, in vivo. Oncolytic adenovirus is a promising therapy for the treatment of solid tumor [19]. Compared with other types of oncolytic virus, its large capacity makes it an ideal vector to carry therapeutic agents [20]. However, the receptor of adenovirus, CXAR, is usually downregulated on the membrane of tumor cells, leading to reduced viral replication and infectivity for tumor tissue as confirmed in previous researches, which restrain its utility as monotherapy [21]. According to our results, the oAD-IL7 successfully infected all of the glioblastoma cell lines and resulted in the apoptosis of tumor cells in vitro, but failed to induce a significant and persistent anti-tumor efficacy when used alone in xenograft models as the mice treated with oAD-IL7 did not present significantly prolonged survival. This limited anti-tumor efficacy of oAD-IL7 may be attributed to the tumor heterogeneity which leads to the down-regulation of CXAR and the innate anti-virus immunity of the mice which leads to increased viral eradication and reduced viral infection in tumor.

We constructed a B7H3-targeted CAR-T and confirmed that the B7H3-CAR-T underwent improved proliferation and survival in vitro with the existence of oAD-IL7. B7H3 is a promising target discovered in recent years prevailing in different types of tumors [22, 23]. During our previous research, we certified the therapeutic efficacy of B7H3-targeted CAR-T in treating glioblastoma and hematological cancers [24]. Taking use of improved transduction protocols, we elevated the transduction efficiency of T cells to over 60% CAR⁺. When used with oAD-IL7, the enhanced B7H3-CAR-T performance were attributed, at least partly,

to the IL7 released from the oAD-IL7-infected tumor cells. The B7H3-CAR-T in combined group did not outperform the CAR-T used as single therapy on the third day of cocultivation, but at the end of the second round of cocultivation, the day 7, the former presented significantly improved proliferation according to the CytoTell analysis. This may be explained by the fact that CD3 and CD28 signals indeed induce a thorough activation of T cells, and IL7 is related to the long-term persistence of CAR-T cells and is responsive to the results of previous study of auto-secreting IL7 equipped CAR-T cells [14].

We further explored the combined therapeutic efficacy of oAD-IL7 and B7H3-CAR-T in xenograft models, and the outcomes were consistent with the *in vitro* coculture results. During our research, the single use of B7H3-CAR-T induced a significant tumor regression, but the tumor eventually revived, resulting in the death of the mice during the course of the treatment. This limited therapeutic efficacy of CAR-T therapy for solid tumors has been widely reported in previous researches that the CAR-T cells lose their anti-tumor capability due to the progress of tumor heterogeneity and the immunosuppressive tumor microenvironment [25, 26]. While compared to its counterpart, the combined therapy led to a complete eradication of the tumors, and four out of five treated mice remain survived by the end of the experiment. Besides, according to the results of delayed treatment, when used together with oAD-IL7, the tumor-infiltrating B7H3-CAR-T outnumbered its counterpart by 4 times. We also observed that when used with oAD-IL7, the tumor-infiltrating T cells presented elevated PD1 and LAG-3 expression. This result has also been observed in previous study, such as using IL12-loaded oncolytic vaccinia, IL2-loaded oncolytic adenovirus, or bispecific antibody-loaded oncolytic adenovirus [27–29]. Other than T cells exhaustion, this result has been widely reported and was regarded as a sign of increased activation of tumor-infiltrating T cells. Finally, the improved proliferation of tumor-infiltrating T cells was indicated by elevated ki67 expression. All of these results explained that the improved therapeutic efficacy of the combined use of oAD-IL7 and B7H3-CAR-T were to some extent led by the improved activation and proliferation of the tumor-infiltrating T cells, but not simply because of the dual cytotoxicity of the oAD-IL7 and B7H3-CAR-T.

To provide tumor-infiltrating CAR-T cells with different types of interleukins is an effective way to improve the therapeutic efficacy of CAR-T against solid tumor. During previous research, CAR-T cells equipped with auto-secreted IL7 or IL7R were proved to be significantly improved for the treatment of solid tumor [13, 14]. However, when T cells are equipped with such consistent growth factor signal, there is a risk for the T cell to undergo intensified off-target side effect due to its target-dispensable over-proliferation [30]. Meanwhile, the use of oncolytic virus has been proved to be a safe

and effective way to carry immuno-activating agents into solid tumor, such as bispecific antibody, immune-checkpoint inhibitor, and interleukins. In our study, we used an oncolytic adenovirus to ensure that the IL7 mainly distributed in the tumor microenvironment, which also avoided extra manipulation of T cells. However, there are also two major limitations of our study. The first is that the E1A gene of our oncolytic adenovirus is under the control of an hTERT promoter, which hinders the oAD-IL7 from replicating in and thus induced a cytotoxicity effect for the mouse-derived glioblastoma cells, such as GL261. The second one is that our B7H3-CAR-T is based on a humanized anti-B7H3 scfv, which can only induce cytotoxicity to human-derived cancer cell lines. Both the limitations restrained our xenograft models to the immuno-deficient NCG mice, which failed to present intact immuno-activating profile of the oAD-IL7 and prevented us from observing the bystander anti-tumor effect and the construction of long-term immune surveillance after the eradication of tumors reported during previous research.

Conclusion

To conclude, we have shown that the combined use of oAD-IL7 and B7H3-CAR-T displayed synergistic anti-tumor effects *in vitro* and *in vivo* by enhancing T cell persistence, which led to prolonged survival of the tumor-bearing mice. These data laid a solid foundation for the further clinical study of the combination therapy for glioblastoma treatment.

Supplementary information The online version of this article (<https://doi.org/10.1007/s00262-021-02856-0>) contains supplementary material, which is available to authorized users.

Acknowledgements We thank Sheng Zenghua for the gift of H4 cell type. We also thank Cao Yi for the gift of glioblastoma tissue acquired from patients.

Author contributions LZ raised the idea. JH designed the experiment and completed it with MZ. ZZ contributed to the xenograft model construction. XT and YC drafted the manuscript. AP completed the statistics analysis, and AT and XP revised the manuscript.

Funding This work was supported by the National Natural Science Foundation of China (31471286 and 81772693), the National Major Scientific and Technological Special Project for Significant New Drugs Development (2015ZX09102010), the Postdoctoral Research Fund of Sichuan University (2018SCU12035), and Technology Innovation Project of Chengdu Science and Technology Bureau (No. 2019-YF05-00459-SN).

Availability of data and material All of the data relevant to this research are included in the article and supplementary files. Materials are available from corresponding author under reasonable request.

Compliance with ethical standards

Conflict of interest The authors declare that they have no conflict of interest.

Ethics approval and consent to participate All animal experiments followed a protocol approved by the Institutional Animal Care and Use Committee of Sichuan University.

Patient consent for publication Not required.

References

- Pagel JM, West HJ (2017) Chimeric antigen receptor (CAR) T-cell therapy. *JAMA Oncol* 11:1595
- Calmes-Miller J (2018) FDA approves second CAR T-cell therapy. *Cancer Discov* 1:5–6
- Li J, Li W, Huang K, Zhang Y, Kupfer G, Zhao Q (2018) Chimeric antigen receptor T cell (CAR-T) immunotherapy for solid tumors: lessons learned and strategies for moving forward. *J Hematol Oncol* 1:22
- Hegde PS, Chen DS (2020) Top 10 challenges in cancer immunotherapy. *Immunity* 1:17–35
- Grosser R, Cherkassky L, Chintala N, Adusumilli PS (2019) Combination immunotherapy with CAR T cells and checkpoint blockade for the treatment of solid tumors. *Cancer Cell* 5:471–482
- Ma X, Shou P, Smith C, Chen Y, Du H, Sun C, Porterfield Kren N, Michaud D, Ahn S, Vincent B et al (2020) Interleukin-23 engineering improves CAR T cell function in solid tumors. *Nat Biotechnol* 4:448–459
- Harrington K, Freeman DJ, Kelly B, Harper J, Soria JC (2019) Optimizing oncolytic virotherapy in cancer treatment. *Nat Rev Drug Discov* 9:689–706
- Hemminki O, Dos Santos JM, Hemminki A (2020) Oncolytic viruses for cancer immunotherapy. *Journal of Hematol Oncol* 1:84
- Twumasi-Boateng K, Pettigrew JL, Kwok YYE, Bell JC, Nelson BH (2018) Oncolytic viruses as engineering platforms for combination immunotherapy. *Nat Rev Cancer* 7:419–432
- Ge Y, Wang H, Ren J, Liu W, Chen L, Chen H, Ye J, Dai E, Ma C, Ju S et al (2020) Oncolytic vaccinia virus delivering tethered IL-12 enhances antitumor effects with improved safety. *J Immunother Cancer* 8(1):e000710
- Nakao S, Arai Y, Tasaki M, Yamashita M, Murakami R, Kawase T, Amino N, Nakatake M, Kurosaki H, Mori M et al (2020) Intratumoral expression of IL7 and IL-12 using an oncolytic virus increases systemic sensitivity to immune checkpoint blockade. *Sci Transl Med*. <https://doi.org/10.1126/scitranslmed.aax7992>
- Perna SK, Pagliara D, Mahendravada A, Liu H, Brenner MK, Savoldo B, Dotti G (2014) Interleukin-7 mediates selective expansion of tumor-redirectioned cytotoxic T lymphocytes (CTLs) without enhancement of regulatory T-cell inhibition. *Clin Cancer Res* 1:131–139
- Shum T, Omer B, Tashiro H, Kruse RL, Wagner DL, Parikh K, Yi Z, Sauer T, Liu D, Parihar R et al (2017) Constitutive signaling from an engineered IL7 receptor promotes durable tumor elimination by tumor-redirectioned T cells. *Cancer Discov* 11:1238–1247
- Adachi K, Kano Y, Nagai T, Okuyama N, Sakoda Y, Tamada K (2018) IL7 and CCL19 expression in CAR-T cells improves immune cell infiltration and CAR-T cell survival in the tumor. *Nat Biotechnol* 4:346–351
- Tang X, Zhao S, Zhang Y, Wang Y, Zhang Z, Yang M, Zhu Y, Zhang G, Guo G, Tong A et al (2019) B7–H3 as a novel CAR-T therapeutic target for glioblastoma. *Mol Ther Oncol* 14:279–287
- Li X, Liu Y, Wen Z, Li C, Lu H, Tian M, Jin K, Sun L, Gao P, Yang E et al (2010) Potent anti-tumor effects of a dual specific oncolytic adenovirus expressing apoptin in vitro and in vivo. *Mol Cancer* 9:10
- Mescher MF, Curtsinger JM, Agarwal P, Casey KA, Gerner M, Hammerbeck CD, Popescu F, Xiao Z (2006) Signals required for programming effector and memory development by CD8+ T cells. *Immunity* 21:81–92
- Zhou J, Jin L, Wang F, Zhang Y, Liu B, Zhao T (2019) Chimeric antigen receptor T (CAR-T) cells expanded with IL7/IL-15 mediate superior antitumor effects. *Protein Cell* 10:764–769
- Sidaway P (2018) CNS cancer: Oncolytic adenovirus effective in patients with glioblastoma. *Nat Rev Clin Oncol* 5:266
- Qian C, Liu XY, Prieto J (2006) Therapy of cancer by cytokines mediated by gene therapy approach. *Cell Res* 2:182–188
- Wing A, Fajardo CA, Posey AD, Shaw C, Da T, Young RM, Alemany R, June CH, Guedan S (2018) Improving CART-Cell Therapy of Solid Tumors with Oncolytic Virus-Driven Production of a Bispecific T-cell Engager. *Cancer Immunol Res* 5:605–616
- Majzner RG, Theruvath JL, Nellan A, Heitzeneder S, Cui Y, Mount CW, Rietberg SP, Linde MH, Xu P, Rota C et al (2019) CAR T cells targeting B7–H3, a pan-cancer antigen, demonstrate potent preclinical activity against pediatric solid tumors and brain tumors. *Clin Cancer Res* 8:2560–2574
- Flem-Karlsen K, Fodstad Ø, Tan M, Nunes-Xavier CE (2018) B7–H3 in cancer—beyond immune regulation. *Trends in Cancer* 6:401–404
- Zhang Z, Jiang C, Liu Z, Yang M, Tang X, Wang Y, Zheng M, Huang J, Zhong K, Zhao S et al (2020) B7-H3-Targeted CAR-T Cells Exhibit Potent Antitumor Effects on Hematologic and Solid Tumors. *Mol Ther Oncol* 17:180–189
- Brown CE, Alizadeh D, Starr R, Weng L, Wagner JR, Naranjo A, Ostberg JR, Blanchard MS, Kilpatrick J, Simpson J et al (2016) Regression of glioblastoma after chimeric antigen receptor T-cell therapy. *New Engl J Med* 26:2561–2569
- Ahmed N, Brawley V, Hegde M, Bielamowicz K, Kalra M, Landi D, Robertson C, Gray TL, Diouf O, Wakefield A et al (2017) HER2-specific chimeric antigen receptor-modified virus-specific T cells for progressive glioblastoma: a phase 1 dose-escalation trial. *JAMA Oncol* 8:1094–1101
- Cervera-Carrascon V, Siurala M, Santos JM, Havunen R, Tähtinen S, Karell P, Sorsa S, Kanerva A, Hemminki A (2018) TNF α and IL-2 armed adenoviruses enable complete responses by anti-PD-1 checkpoint blockade. *Oncoimmunology* 5:e1412902
- Wang P, Li X, Wang J, Gao D, Li Y, Li H, Chu Y, Zhang Z, Liu H, Jiang G et al (2017) Re-designing Interleukin-12 to enhance its safety and potential as an anti-tumor immunotherapeutic agent. *Nat Commun* 1:1395
- Fajardo CA, Guedan S, Rojas LA, Moreno R, Arias-Badia M, de Sostoa J, June CH, Alemany R (2017) Oncolytic adenoviral delivery of an EGFR-targeting T-cell engager improves antitumor efficacy. *Can Res* 8:2052–2063
- Porter CE, Rosewell Shaw A, Jung Y, Yip T, Castro PD, Sandulache VC, Sikora A, Gottschalk S, Ittman MM, Brenner MK et al (2020) Oncolytic adenovirus armed with BiTE, cytokine, and checkpoint inhibitor enables CAR T cells to control the growth of heterogeneous tumors. *Mol Ther* 5:1251–1262
- Ahmed M, Cheng M, Zhao Q, Goldgur Y, Cheal SM, Guo HF, Larson SM, Cheung NK (2015) Humanized affinity-matured monoclonal antibody 8H9 has potent antitumor activity and binds to FG loop of tumor antigen B7–H3. *J Biol Chem* 290(50):30018–30029. <https://doi.org/10.1074/jbc.M115.679852>

Publisher's Note Springer Nature remains neutral with regard to jurisdictional claims in published maps and institutional affiliations.